

Storage and Release of Soluble Hexavalent Chromium from Chromate Conversion Coatings

Equilibrium Aspects of Cr^{VI} Concentration

Lin Xia,^a Ejii Akiyama,^b Gerald Frankel,^{b,*} and Richard McCreery^{a,*,z}

^aDepartment of Chemistry and ^bDepartment of Materials Science and Engineering, The Ohio State University, Columbus, Ohio 43210, USA

The release of soluble Cr^{VI} species by a chromate conversion coating (CCC) was monitored quantitatively by ultraviolet-visible spectroscopy. By careful selection of measurement wavelength (339 nm), the Cr^{VI} concentration could be determined without regard to solution pH or Cr^{VI} speciation. The Cr^{VI} concentration in solution over a CCC reached an equilibrium value that depended on pH, ionic strength, and the ratio of the CCC surface area to the solution volume (A/V). In separate experiments, the adsorption of Cr^{VI} by synthetic Cr^{III} hydroxide to form a Cr^{III}-Cr^{VI} mixed oxide was observed, and also led to an equilibrium concentration of Cr^{VI} in solution. The equilibrium Cr^{VI} concentration was determined for a variety of A/V values on both AA1100 and AA2024-T3 aluminum alloys. The results are inconsistent with release mechanisms based on the solubility of a Cr^{VI} salt in the solution or depletion of Cr^{VI} from the CCC. However, the observed concentrations are consistent with a mechanism similar to a Langmuirian adsorption-desorption equilibrium of Cr^{VI} on a porous, insoluble Cr^{III} hydroxide matrix. The Cr^{III} hydroxide matrix has a finite number of Cr^{VI} binding sites and exhibits a nonlinear relationship between solution and solid Cr^{VI} concentrations governed by an equation similar to a Langmuir adsorption isotherm. The proposed model incorporates reversible adsorption and desorption of Cr^{VI}, with adsorption favored at low pH during formation of the CCC, and desorption favored in field conditions. The model quantitatively predicts the observed concentrations after determining the binding constant from fits to the data. The model explains the capacity of a CCC to release active Cr^{VI} corrosion inhibitor and provides strong evidence that Cr^{VI} storage in a CCC involves reversible formation of a Cr^{VI}-O-Cr^{III} mixed oxide.

© 2000 The Electrochemical Society. S0013-4651(99)11-058-9. All rights reserved.

Manuscript submitted November 15, 1999; revised manuscript received April 7, 2000.

It is generally accepted that Cr^{VI} in chromate conversion coatings (CCCs) and in SrCrO₄ containing primers^c is the critical component in corrosion protective coating systems used on aluminum aircraft alloys such as AA-2024-T3. The ability of a CCC to release Cr^{VI} as soluble chromate species is likely to be important to "self-healing" exhibited by CCCs, in which CrO₄²⁻ or related species can migrate to defects or corrosion sites and inhibit further damage.¹⁻⁸ Several investigators have reported that CCCs contain both Cr^{III} and Cr^{VI}⁹⁻¹¹ and a Cr^{III}-Cr^{VI} mixed oxide has been identified as a major CCC component.¹² Furthermore, release of CrO₄²⁻ from a CCC has been demonstrated, as has protection of an initially untreated alloy surface by dilute CrO₄²⁻ in a chloride solution.⁷ The mechanism of corrosion protection by chromate is currently being debated, but storage and release of Cr^{VI} by a CCC appear to be essential for its long term protection property. In addition, release of chromate from sparingly soluble SrCrO₄ in primers may also provide a source of dilute chromate for self-healing.

The current investigation addresses the storage and release of Cr^{VI} in more detail. The release of Cr^{VI} from a CCC and SrCrO₄ into water and salt solution was monitored quantitatively with ultraviolet-visible (UV-vis) spectroscopy, in order to examine solution concentrations, saturation (if any), release rate, and possibly storage mechanism. By considering a variety of conditions, a quantitative model for Cr^{VI} storage and release was formulated, and its implications for corrosion protection were considered. The kinetics and rate-controlling factors during release will be addressed in a separate communication.

Experimental

All the chemicals used were analytical grade. Solutions were prepared with "deionized" water (Barnstead, Nanopure 18 MΩ-cm). The absorbance vs. concentration behavior of chromate solutions is complicated by the equilibria between HCrO₄⁻, CrO₄²⁻, and Cr₂O₇²⁻, which depend on both concentration and pH.¹³⁻¹⁷ The combined

concentration of these species in solution is indicated herein as [Cr^{VI}]. In order to determine the relationship between UV-vis absorbance and [Cr^{VI}], solutions of K₂Cr₂O₇ were prepared at various concentrations in the range of 1.0×10^{-5} M to 4×10^{-4} M of Cr^{VI}, and adjusted to different pH values with HClO₄ or NaOH and a pH meter. UV-vis absorption spectra for solutions in 1 cm quartz cuvettes were collected using either a Perkin Elmer Lambda 20 spectrometer or a custom system based on an ISA Triax monochromator. Spectra for one Cr^{VI} concentration are shown in Fig. 1 for a pH range from 2.01-9.47. Since the absorption at 339 nm (A_{339}) was independent of pH, this wavelength was used to construct the pH-independent calibration curve shown in Fig. 2. The absorbance at 339 nm was preferable to that at 295 nm for quantitative analysis of [Cr^{VI}] due to the smaller interference from nitrate ion. Over the range of total [Cr^{VI}] from 1×10^{-5} to 4×10^{-4} M and pH range 2.0 to 9.5, A_{339} is linear with total [Cr^{VI}]. This calibration curve was used to

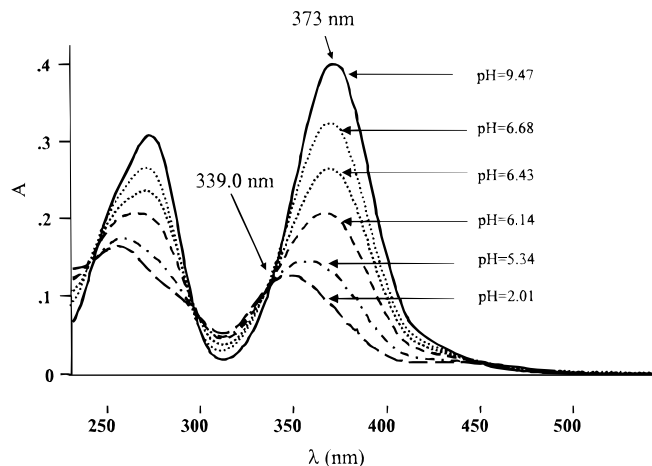


Figure 1. UV-vis spectra of 8.3×10^{-5} M Cr^{VI} as a function of pH. Path length was 1 cm. A is the observed absorbance.

* Electrochemical Society Active Member.

^z E-mail: mcCreery.2@osu.edu

^c Roman numerals are used to indicate oxidation state, as in Cr^{VI}. Arabic numerals denote ionic charge, as in CrO₄²⁻.

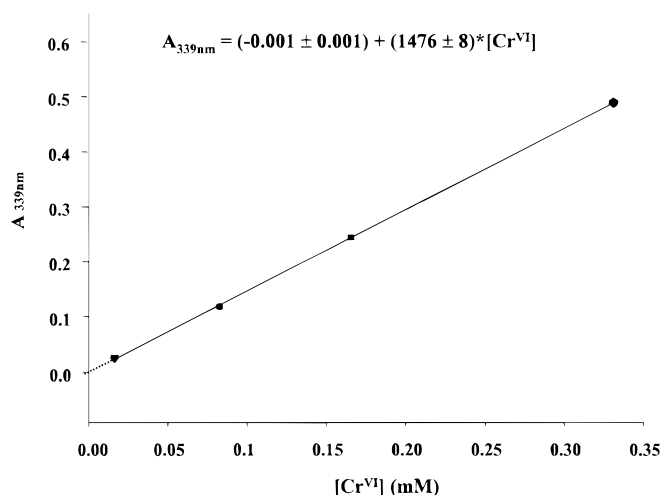


Figure 2. Calibration line of $A_{339\text{nm}}$ vs. total Cr^{VI} concentration. The $8.3 \times 10^{-5} \text{ M}$ point (·) is the average of 12 samples with the same $[\text{Cr}^{\text{VI}}]$, but pH 2.01-9.47. All other points are the average of four samples with the same $[\text{Cr}^{\text{VI}}]$ concentration, but pH 5-6.

determine $[\text{Cr}^{\text{VI}}]$ from observed A_{339} in subsequent experiments. The molar absorptivity in terms of total Cr^{VI} concentration is $1.48 \times 10^5 \text{ M}^{-1} \text{ cm}^{-1}$ at 339 nm over the pH range 2-9.5.

Cr^{VI} concentrations in solution were determined spectrophotometrically as a function of time for several starting conditions, including a CCC in water or salt solution, $\text{Cr}^{\text{III/VI}}$ mixed oxide in water, and Cr^{III} hydroxide immersed in dilute Cr^{VI} solution. CCC films were prepared by dipping polished AA2024-T3 alloy or AA1100 alloy (polished with $\text{Al}_2\text{O}_3/\text{H}_2\text{O}$ slurries as described in Ref. 7) into freshly prepared Alodine coating solution (Alodine 1200, 7.5 g/L, pH 1.3) at room temperature for 1 min, washing with more than 100 mL flowing water, and then air drying for various periods of time (indicated below). Then the coupons were immersed in a known volume of deionized water or 0.1 M NaCl, in well-sealed glass containers. $\text{Cr}^{\text{III}}\text{-Cr}^{\text{VI}}$ mixed-oxide was prepared as described previously.¹² A known weight of freshly prepared $\text{Cr}^{\text{III}}\text{-Cr}^{\text{VI}}$ mixed-oxide was weighed and dried on a small piece of glass in air for known periods of time. The dried $\text{Cr}^{\text{III}}\text{-Cr}^{\text{VI}}$ mixed-oxide powder samples on glass were immersed in known volumes of Nanopure water or 0.1 M NaCl solution and tightly covered. The containers were agitated occasionally over a period of several days. Aliquots (2-3 mL) of each solution were withdrawn periodically for UV-vis spectroscopy, then returned to the corresponding container. $[\text{Cr}^{\text{VI}}]$ released from the CCC film or mixed oxides was determined from the absorbance at 339.0 nm. The details of CCC surface/volume ratio and $\text{Cr}^{\text{III}}\text{-Cr}^{\text{VI}}$ mixed-oxide mass/volume ratio are listed in Table I.

Saturation concentrations of SrCrO_4 in deionized water or 0.1 M NaCl were obtained by adding 2 g of SrCrO_4 to 100 ml Nanopure water or 0.1 M NaCl, and stirring for 6 days. After centrifugation, 1.00 mL of supernatant was diluted to 50.00 mL with 2 M NaOH,

Table I. Observed equilibrium Cr^{VI} concentration in solution under various conditions.

Material (2024-T3 unless indicated otherwise)	Aging time (h)	A/V or m/V (cm ² /mL) or (g/mL) ^a	Solution	Equilibrium Cr^{VI} in solution (M) ^b
CCC on AA2024-T3	0	0.4	Deionized water	6.0×10^{-5}
CCC on AA2024-T3	0	0.8	Deionized water	1.2×10^{-4}
CCC on AA2024-T3	0	1.2	Deionized water	1.7×10^{-4}
CCC on AA1100	2	1.67	Deionized water	2.0×10^{-4}
				2.1×10^{-4}
				2.3×10^{-4}
CCC on AA1100	2	5.0	Deionized water	6.5×10^{-4}
				6.9×10^{-4}
				5.6×10^{-4}
CCC on AA1100	2	10.0	Deionized water	8.2×10^{-4}
				9.0×10^{-4}
CCC on AA1100	2	20.0	Deionized water	1.22×10^{-3}
CCC on AA2024-T3	0.25	4.5	Deionized water	1.34×10^{-4}
CCC on AA2024-T3	22	4.5	Deionized water	1.54×10^{-4}
CCC on AA2024-T3	96	4.5	Deionized water	1.32×10^{-4}
CCC on AA2024-T3	210	4.5	Deionized water	1.16×10^{-4}
CCC on AA2024-T3	22	4.5	0.1 M NaCl solution	1.94×10^{-4}
CCC on AA2024-T3	2	1.67	Deionized water	1.0×10^{-4}
CCC on AA2024-T3	2	5.0	Deionized water	3.6×10^{-4}
$\text{Cr}^{\text{III}}\text{-Cr}^{\text{VI}}$ mixed-oxide	0.25	0.0032	Deionized water	2.11×10^{-4}
$\text{Cr}^{\text{III}}\text{-Cr}^{\text{VI}}$ mixed-oxide	22	0.0032	Deionized water	1.56×10^{-4}
$\text{Cr}^{\text{III}}\text{-Cr}^{\text{VI}}$ mixed-oxide	96	0.0032	Deionized water	1.33×10^{-4}
$\text{Cr}^{\text{III}}\text{-Cr}^{\text{VI}}$ mixed-oxide	210	0.0032	Deionized water	1.28×10^{-4}
$\text{Cr}^{\text{III}}\text{-Cr}^{\text{VI}}$ mixed-oxide	0.25	0.0032	0.1 M NaCl solution	2.97×10^{-4}
$\text{Cr}^{\text{III}}\text{-Cr}^{\text{VI}}$ mixed-oxide	22	0.0032	0.1 M NaCl solution	2.92×10^{-4}
$\text{Cr}^{\text{III}}\text{-Cr}^{\text{VI}}$ mixed-oxide	0.25	0.00092	Deionized water	4.03×10^{-4}
$\text{Cr}^{\text{III}}\text{-Cr}^{\text{VI}}$ mixed-oxide	0.25	0.00092	Deionized water	4.48×10^{-4}
$\text{Cr}^{\text{III}}\text{-Cr}^{\text{VI}}$ mixed-oxide	0.25	0.0013	Deionized water	2.70×10^{-4}
$\text{Cr}^{\text{III}}\text{-Cr}^{\text{VI}}$ mixed-oxide	0.25	0.0017	Deionized water	5.33×10^{-4}
$\text{Cr}^{\text{III}}\text{-Cr}^{\text{VI}}$ mixed-oxide	0.25	0.0020	Deionized water	6.85×10^{-4}
$\text{Cr}^{\text{III}}\text{-Cr}^{\text{VI}}$ mixed-oxide	0.25	0.0030	Deionized water	7.66×10^{-4}
$\text{Cr}^{\text{III}}\text{-Cr}^{\text{VI}}$ mixed-oxide	0.25	0.0037	Deionized water	9.39×10^{-4}
$\text{Cr}^{\text{III}}\text{-Cr}^{\text{VI}}$ mixed-oxide	0.25	0.0042	Deionized water	9.81×10^{-4}
SrCrO_4	N/A	0.020	Deionized water	4.65×10^{-3}
SrCrO_4	N/A	0.020	0.1 M NaCl solution	7.81×10^{-3}

^a A/V is the ratio of CCC film area to solution volume, m/V is the ratio of mixed oxide weight to solution volume.

^b Cr^{VI} concentration observed after reaching an apparently constant value, at least 10 days after immersion.

Table II. Equilibrium Cr^{VI} concentration in solution after adsorption to Cr^{III}-hydroxide.

[Cr ^{VI}] _{t=0} (mM)	Mass of Cr(OH) ₃ (g, in 50 mL solution)	Initial pH	[Cr ^{VI}] _{final} (mM)	[Cr ^{VI}] _{t=0} - [Cr ^{VI}] _{final} (mM)
10.17	1.051	7.19	8.939	1.231
10.17	0.1075	7.19	9.936	0.2340
10.12	1.309	2.76	6.558	3.562
10.12	0.1408	2.76	9.380	0.740
0.937	1.003	7.59	0.5108	0.4259
0.937	0.1563	7.59	0.8369	0.0998
0.947	1.051	2.67	0.0842	0.8595
0.947	0.1075	2.67	0.4621	0.4816
0.112	1.020	7.66	0.01997	0.09243
0.112	0.1321	7.66	0.011	0.1014
0.117	1.008	2.58	0.04097	0.07603
0.117	0.1076	2.58	0.04347	0.07353
10.14	0.2942	7.19	9.430	0.710
10.14	0.5169	7.19	9.182	0.958
10.14	0.8238	7.19	8.835	1.305
10.14	0.3216	2.67	8.531	1.609
10.14	0.5077	2.67	7.661	2.479
10.14	0.8146	2.67	6.324	3.816
10.14	2.8885	7.19	6.598	3.542
10.14	3.6067	7.19	5.002	5.138
10.14	6.0380	7.19	3.245	6.895
10.14	2.7110	2.67	2.412	7.728
10.14	3.9886	2.67	1.736	8.404
10.14	3.9886	2.67	1.736	8.404
10.14	5.7103	2.67	0.5566	9.5834
5.91	1.0046	2.68	1.749	4.156
5.91	1.1340	7.18	4.189	1.716
3.01	1.0421	2.71	0.1383	2.8677
3.01	1.1022	7.18	1.701	1.305

then a UV-vis spectrum was obtained. The CrO₄²⁻ concentration was determined from the molar absorptivity at 373 nm, 4884 M⁻¹ cm⁻¹. For experiments in which the sample was not reused, such as SrCrO₄ saturation and the pH effects described below, it was more convenient to dilute the sample with NaOH and determine the absorbance at 373 rather than 339 nm. This approach significantly reduced possible interference from NO₃⁻.

The adsorption of aqueous Cr^{VI} by Cr^{III}-hydroxide was studied by adding [Cr^{VI}] solution to solid Cr(OH)₃ prepared as described previously.¹² A known amount (0.1 to 1.0 g) of Cr(OH)₃ was combined with 50.0 mL of [Cr^{VI}] solution with known concentration and pH in a sealed vial which was shaken occasionally thereafter. Aliquots of solution were withdrawn periodically, centrifuged, quantitatively diluted with 2 M NaOH, and analyzed spectrophotometrically at 373 nm. Details about the mass of Cr^{III}-hydroxide and initial/final [Cr^{VI}] are listed in Table II.

The dynamic interaction between Cr^{III}-hydroxide and Cr^{VI} was studied as follows. A mixture of 0.062 M (as Cr(NO₃)₃·9H₂O) and 0.019 M Cr^{VI} (as K₂Cr₂O₇) was prepared. The total volume was 500 mL and the initial pH was below 3. In the first cycle, concentrated (~20 M) NaOH was added dropwise while agitating the solution. After each NaOH addition, the solution was stirred until the pH stabilized to ±0.1 pH unit. 10 mL of the suspension was centrifuged for 5 min, then 1.00 mL aliquot of supernatant solution was quantitatively diluted to 50.00 mL by 2 M NaOH and analyzed spectrophotometrically. The remaining supernatant solution and solid was returned to the original 500 mL volume of solution. NaOH was added repeatedly such that spectra were obtained at 0.5–1.0 pH unit increments. Spectra were obtained after aliquots were diluted with NaOH, since the NO₃⁻ band (310 nm) overlaps with Cr^{VI} bands at acidic or neutral pH. After reaching a pH of 12, the process was reversed by incremental addition of concentrated HNO₃ until the pH was less

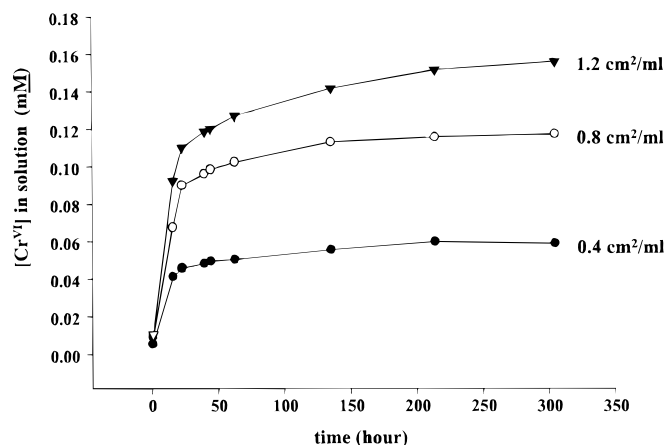


Figure 3. Cr^{VI} concentration determined from the absorbance at 339 nm as a function of time after immersion of a CCC in nanopure water. Curves are labeled with the ratio of the geometric CCC area to solution volume.

than 3. A second complete cycle of NaOH and HNO₃ addition was conducted, in order to demonstrate reversibility. A similar experiment was carried out by using Cr₂O₃, instead of Cr(NO₃)₃·9H₂O.

Results

When a CCC was immersed in water or salt solution, the Cr^{VI} concentration in solution increased with time, as shown in Fig. 3. The Cr^{VI} is a mixture of CrO₄²⁻, Cr₂O₇²⁻, and HCrO₄⁻, depending on concentration and pH, but the absorbance at 339 nm permits assessment of total Cr^{VI} in solution. All release curves of the type shown in Fig. 3 eventually reached a constant Cr^{VI} concentration after several days, and these limiting concentrations are listed in Table I for a variety of initial conditions. Several observations deserve special note. First, a higher ratio of CCC area to solution volume led to higher [Cr^{VI}] in solution. Second, aging of the CCC before exposure to water decreased the final [Cr^{VI}], but not greatly. Third, the [Cr^{VI}] observed in 0.1 M NaCl was higher than that in deionized water, by approximately 26%, as shown in Fig. 4.

Release of Cr^{VI} from Cr^{III}-Cr^{VI} mixed oxide was studied by adding known weights of synthetic mixed oxide to known volumes of water or salt solution, followed by spectrophotometric monitoring. Release curves similar to those of Fig. 3 and 4 were observed, and the final concentrations are listed in Table I. As was the case with the CCC, the final [Cr^{VI}] after release from the synthetic mixed oxide was in the range of 10⁻⁴ to 10⁻³ M, decreased with aging time, and was slightly higher in 0.1 M NaCl than in water. Table I also lists the final concentration of [Cr^{VI}] released from solid SrCrO₄

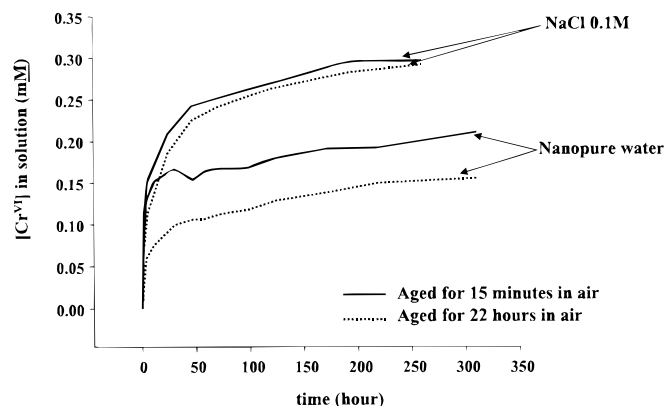
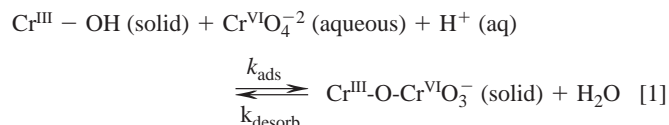


Figure 4. [Cr^{VI}] vs. time curves for Cr^{III}-Cr^{VI} mixed oxide immersed in nanopure water or 0.1 M NaCl. 3.2 mg of mixed oxide was present per milliliter of solution, and then aged for the periods indicated.

into water and 0.1 M NaCl. For both the mixed oxide and SrCrO_4 , solid remained after reaching the final $[\text{Cr}^{\text{VI}}]$ level. The ratio of the final $[\text{Cr}^{\text{VI}}]$ observed in water to that in 0.1 M NaCl ranged from 0.60 for SrCrO_4 , 0.5-0.7 for the CCC, to 0.79 for the mixed oxide. This ratio did vary somewhat with aging time and A/V ratio, but was consistently in the range of 0.6 to 0.8 for all three starting materials. The activity coefficient of the dominant Cr^{VI} species in solution (HCrO_4^-) in 0.1 M NaCl is 0.769, calculated from the extended Debye-Huckle equation.¹³ The experimental ratios are very close to this calculated value, implying that the higher concentration observed in NaCl is due to a reduced activity coefficient.

If the constant $[\text{Cr}^{\text{VI}}]$ observed at long times in Fig. 3 and 4 represents an equilibrium between solution and solid Cr^{VI} , then Cr^{III} oxide should adsorb Cr^{VI} from solution, according to Reaction 1



Reaction 1 is a simplified form of a reaction proposed in a previous report to represent a dynamic equilibrium between the $\text{Cr}^{\text{III}}\text{-Cr}^{\text{VI}}$ mixed oxide and aqueous Cr^{VI} ,¹² and the remaining bonds to Cr^{III} are not shown to improve clarity. CrO_4^{2-} is used as an example of Cr^{VI} (aq); similar equilibria by using HCrO_4^- (aq), $\text{Cr}_2\text{O}_7^{2-}$ (aq) are also possible. As written, the reverse reaction describes release of Cr^{VI} into solution from the CCC or mixed oxide, while the forward reaction represents Cr^{VI} adsorption by Cr^{III} hydroxide. To test the forward reaction, Cr^{III} hydroxide was added to Cr^{VI} solution, and the Cr^{VI} in solution was monitored spectrophotometrically. Figure 5 and

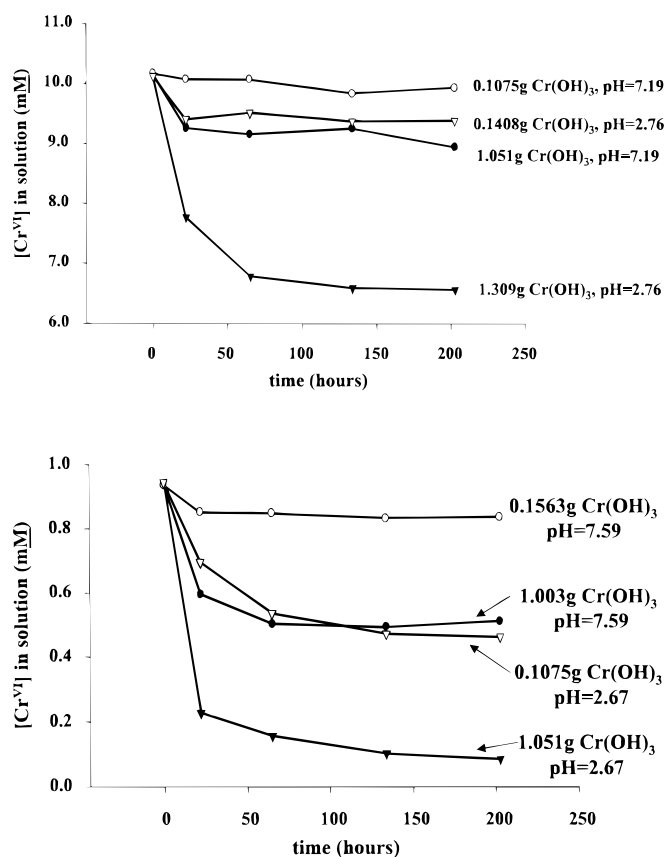


Figure 5. $[\text{Cr}^{\text{VI}}]$ observed over $\text{Cr}^{\text{III}}(\text{OH})_3$ placed in 50 mL of solution which initially contained 10.0 mM $[\text{Cr}^{\text{VI}}]$ (A, top) or 1 mM $[\text{Cr}^{\text{VI}}]$ (B, bottom). The initial pH was adjusted to the value indicated with HNO_3 or NaOH . $\text{Cr}^{\text{III}}(\text{OH})_3$ was prepared freshly, and the weight indicated was added to the Cr^{VI} solution.

Table II show results for Cr^{VI} adsorption by Cr^{VI} hydroxide for different pH values and different initial weights of Cr^{III} hydroxide. The solid $\text{Cr}(\text{OH})_3$ did indeed adsorb Cr^{VI} from solution, and the solution concentration decreased to an apparently constant $[\text{Cr}^{\text{VI}}]$ level. Table II lists several final Cr^{VI} concentrations for different initial conditions. Adsorption was more pronounced at lower pH, and for higher weights of Cr^{III} hydroxide.

The dynamic nature of the equilibrium between dissolved and adsorbed Cr^{VI} was examined further by cycling the pH of a $\text{Cr}^{\text{III}}\text{-Cr}^{\text{VI}}$ solution, as described in the experimental section. As concentrated NaOH was added dropwise, to soluble Cr^{III} and Cr^{VI} salts, the $\text{Cr}^{\text{III}}\text{-Cr}^{\text{VI}}$ mixed oxide formed and was allowed to equilibrate at a given pH for about 2 h. The total $[\text{Cr}^{\text{VI}}]$ was determined spectrophotometrically, and the pH was measured before adding another aliquot of NaOH and re-equilibration at a different pH. After reaching pH 10-12, HNO_3 was added to decrease pH, and two complete pH excursions were carried out in this fashion. A plot of solution $[\text{Cr}^{\text{VI}}]$ vs. pH is shown in Fig. 6. Each point was taken after the addition of concentrated NaOH or HNO_3 and equilibration at a particular pH. A similar experiment starting with solid Cr_2O_3 and Cr^{VI} solution exhibited no adsorption of Cr^{VI} from solution. To assure time for equilibration, the results shown in Fig. 6 were acquired over a period of 7 days.

Cr^{VI} loading levels in $\text{Cr}^{\text{III}}\text{-Cr}^{\text{VI}}$ mixed-oxide or CCC film were measured as described previously.¹² CCC film was dissolved in basic solution, or the $\text{Cr}^{\text{III}}\text{-Cr}^{\text{VI}}$ mixed oxide was dissolved in concentrated HNO_3 , then the pH of both was increased to >12 by adding NaOH . Spectrophotometric measurements show that CCC film (Alodine, 1 min on AA2024-T3) contains $(1.03 \pm 0.17) \times 10^{-7}$ mol $\text{Cr}^{\text{VI}}/\text{cm}^2$ and $\text{Cr}^{\text{III}}/\text{Cr}^{\text{VI}}$ -mixed-oxide contains $(5.46 \pm 0.25) \times 10^{-4}$ mol $\text{Cr}^{\text{VI}}/\text{g}$. Both results are the average of three trials.

Discussion

Before considering the quantitative implications of the observations, some useful conclusions are available about Cr^{VI} storage and release. A simple hypothesis might be that Cr^{VI} is trapped in the CCC as a soluble salt, such as $\text{K}_2\text{Cr}_2\text{O}_7$. In this case, the soluble Cr^{VI} would merely dissolve when the CCC was exposed to solution, and the final $[\text{Cr}^{\text{VI}}]$ in solution would be linear with the A/V ratio. This case is plotted as the depletion model of Fig. 7, for which the CCC (or mixed oxide) is merely a repository of a soluble Cr^{VI} salt. The x axis in Fig. 7 is the number of moles of Cr^{VI} in the CCC or mixed oxide divided by the solution volume, and is proportional to either the CCC area/volume ratio or the $\text{Cr}^{\text{III}}\text{-Cr}^{\text{VI}}$ mixed oxide weight/vol-

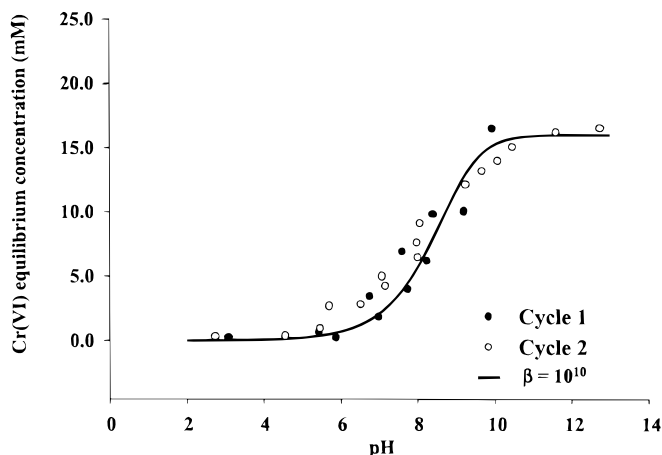


Figure 6. Equilibrium $[\text{Cr}^{\text{VI}}]$ observed for a solution containing 0.062 M $\text{Cr}(\text{NO}_3)_3 \cdot 9\text{H}_2\text{O}$ and 0.019 M Cr^{VI} (as $\text{K}_2\text{Cr}_2\text{O}_7$) following the addition of NaOH , then HNO_3 . The pH was increased from ~ 3 to ~ 10 with NaOH , then decreased to ~ 2.5 with HNO_3 to comprise cycle 1. Open circles indicate the equilibrium $[\text{Cr}^{\text{VI}}]$ for a second complete cycle. Solid line is a fit to Eq. 3 with $\beta = 10^{10}$. See text for details.

ume ratio listed in Table I. This depletion model is inconsistent with the observations for two major reasons. First, the observed $[\text{Cr}^{\text{VI}}]$ is not linear with x in Fig. 7. Second, the uptake of Cr^{VI} by $\text{Cr}(\text{OH})_3$ indicates that Cr^{VI} is not completely soluble in the presence of the synthetic Cr^{III} oxide, or the mixed oxide present in the CCC.

A second possibility is a solubility model, in which the Cr^{VI} concentration over a CCC or the mixed oxide is controlled by a solubility product, analogous to the case for SrCrO_4 . Ignoring reactions of CrO_4^{2-} with H^+ or H_2O , SrCrO_4 should behave as a simple sparingly soluble salt, with a saturation concentration determined by its solubility product ($K_{\text{sp}} = 2.2 \times 10^{-5}$). The behavior of the solubility model is also shown in Fig. 7. Once sufficient Cr^{VI} was available to reach the solubility limit (4.7 mM), the solution would saturate and the addition of more SrCrO_4 would have no further effect on $[\text{Cr}^{\text{VI}}]$ in solution. If the CCC or mixed oxide followed this behavior, we expect a saturation level of Cr^{VI} which could not be exceeded by adding more CCC (increased A/V) or mixed oxide. However, this is not the case, with increasing A/V always resulting in higher $[\text{Cr}^{\text{VI}}]$ in solution. The solubility model is likely to apply to SrCrO_4 contained in the primer, but not to the CCC or the $\text{Cr}^{\text{III}}\text{-Cr}^{\text{VI}}$ mixed oxide.

It is clear that the release of Cr^{VI} from the CCC (or mixed oxide) is reversible and pH dependent, and strongly dependent on the initial amount of Cr^{VI} in the CCC or mixed oxide relative to the solution volume. A mechanism that is consistent with the observations is adsorption of Cr^{VI} species to the insoluble Cr^{III} hydroxide, shown schematically in Fig. 8. We consider the insoluble Cr^{III} to have many surface hydroxyl groups available for formation of $\text{Cr}^{\text{III}}\text{-O-Cr}^{\text{VI}}$ bonds. These hydroxyl groups act as sites for covalent binding of Cr^{VI} according to Eq. 1. $\text{Cr}^{\text{III}}\text{-OH}$ (solid) in Eq. 1 represents insoluble Cr^{III} hydroxide, $\text{Cr}^{\text{VI}}\text{O}_4^{2-}$ (aq) is solution-phase hexavalent chromium, $\text{Cr}^{\text{III}}\text{-O-Cr}^{\text{VI}}$ is the mixed oxide present in the CCC or prepared synthetically depending on pH and concentration. Solution-phase Cr^{VI} may be CrO_4^{2-} , HCrO_4^- , or $\text{Cr}_2\text{O}_7^{2-}$. Reaction 1 is reversible, so the CCC may release Cr^{VI} , and the Cr^{III} hydroxide may adsorb Cr^{VI} from solution. Release and adsorption of Cr^{VI} are pH dependent, favoring the mixed oxide at low pH and soluble Cr^{VI} at higher pH, as observed experimentally (Fig. 6). Furthermore, the number of hydroxyl groups in $\text{Cr}^{\text{VI}}\text{-hydroxide}$ which may be exchanged for Cr^{VI} in finite, resulting in a saturation level of $\text{Cr}^{\text{VI}}\text{:Cr}^{\text{III}}$ of approximately 1:3. The equilibrium for a solution species binding to a finite number of sites on a solid is mathematically similar to Langmuir adsorption behavior as represented by Eq. 2.¹⁸ The insoluble Cr^{VI} oxide is a porous solid containing Cr^{VI} binding sites rather than the flat surface normally associated with Langmuir behavior, but it does exhibit a nonlinear relationship between solution and surface concentration consistent with Eq. 2. If we consider the Cr^{III} oxide matrix in the CCC or mixed

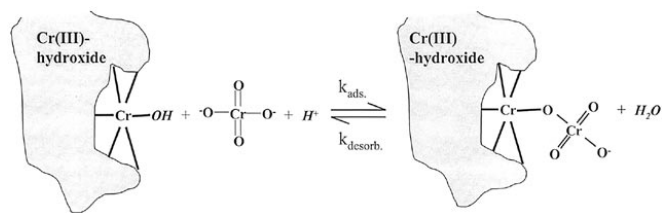


Figure 8. Model for adsorption of Cr^{VI} to solid Cr^{III} hydroxide, based on Eq. 1. Cr^{VI} is shown as CrO_4^{2-} , but may also exist as HCrO_4^- or $\text{Cr}_2\text{O}_7^{2-}$, depending on pH and $[\text{Cr}^{\text{VI}}]$. Gray area represents insoluble Cr^{III} matrix which is permeable by water and solution phase Cr^{VI} .

oxide to have a finite surface area for adsorption with a saturation coverage of adsorbed Cr^{VI} to equal to Γ_s , then

$$\frac{\Gamma_{\text{VI}}}{\Gamma_s - \Gamma_{\text{VI}}} = \beta[\text{Cr}^{\text{VI}}][\text{H}^+] = \frac{\theta_{\text{VI}}}{1 - \theta_{\text{VI}}} \quad [2]$$

where Γ_{VI} is the coverage of Cr^{VI} on the Cr^{III} oxide in mol/cm^2 , β is a binding constant, and θ_{VI} is the fractional coverage of Cr^{VI} . Note that the area relevant to adsorption is the microscopic area of the Cr^{III} oxide matrix, not of the CCC itself. Although this microscopic area is difficult to determine, we assume it to be proportional to the geometric CCC area or to the mass of synthetic mixed oxide. If we define N_{VI} as the moles of Cr^{VI} present in the CCC or mixed oxide solid, N_{VI} may be calculated after assuming a homogeneous distribution of Cr^{VI} in the solid. For the CCC, N_{VI} equals the initial average Cr^{VI} concentration ($\text{mol/geometric cm}^2$) times the CCC geometric area. For the mixed oxide, N_{VI} equals the initial Cr^{VI} loading (mol/gram) times the weight of mixed oxide.

Under the assumption that Eq. 2 controls the Cr^{VI} (aq) concentration of a solution in equilibrium with a CCC or mixed oxide, predictions of the behavior of $[\text{Cr}^{\text{VI}}]$ for several situations may be derived. When Cr^{VI} (aq) is desorbed from an initially saturated CCC or mixed oxide, the $[\text{Cr}^{\text{VI}}]$ follows Eq. 3, with V representing solution volume (see Appendix for derivation)

$$[\text{Cr}^{\text{VI}}]_{\text{equil}} = \frac{-1 + \sqrt{1 + 4\beta[\text{H}^+]N_{\text{VI}}/V}}{2\beta[\text{H}^+]} \quad [3]$$

The observed pH at the end of release experiments was 4.6 ± 0.7 . A fit of Eq. 3 to the equilibrium values of $[\text{Cr}^{\text{VI}}]$ listed in Table I is shown in Fig. 9. Results for the CCC on both AA2024 and AA1100, as well as for the synthetic $\text{Cr}^{\text{III}}\text{-Cr}^{\text{VI}}$ mixed oxide are shown, along

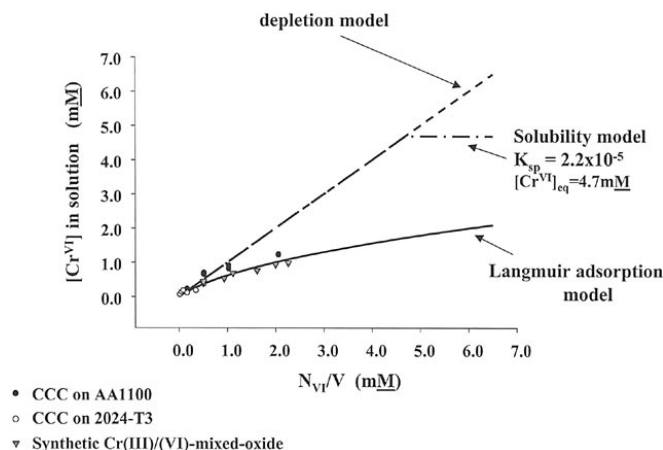


Figure 7. Predicted behavior of $[\text{Cr}^{\text{VI}}]$ as a function of Cr^{VI} loading in a CCC or mixed oxide for the solubility, depletion, and adsorption mechanisms of Cr^{VI} release. N_{VI}/V is the ratio of the moles of Cr^{VI} in the solid to the solution volume. The K_{sp} is that of SrCrO_4 , and is used only to illustrate the shape of the curve.

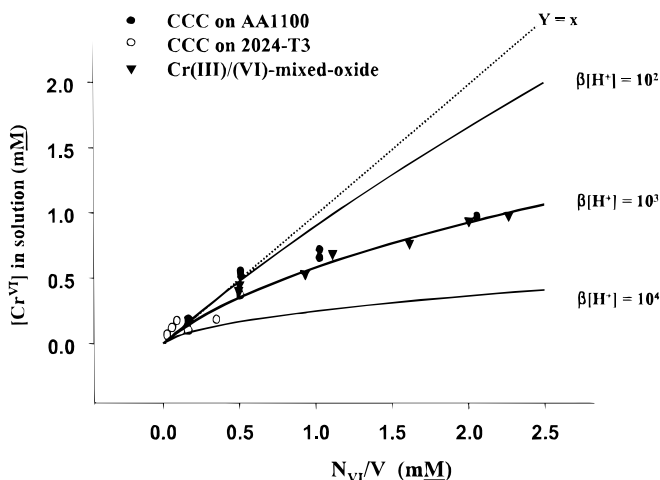


Figure 9. Results of release experiments from a CCC on both AA1100 and AA2024-T3, and the $\text{Cr}^{\text{III}}/\text{Cr}^{\text{VI}}$ mixed oxide. Lines are calculated from Eq. 3 with the indicated values of the product $\beta[\text{H}^+]$. N_{VI}/V is the ratio of adsorbed moles of Cr^{VI} to the solution volume.

with curves predicted from Eq. 3 for three values of the product $\beta[H^+]$. As noted earlier, the model assumes that Cr^{VI} permeates the CCC and is able to adsorb to its microscopic area. This permeation process certainly affects the release kinetics, but Eq. 3 requires only that the entire CCC or mixed oxide has equilibrated with the solution. The release kinetics will be discussed in a separate publication.

The adequate fit of the experimental data to Eq. 3 with $\beta[H^+] = 10^3$ provides support for a saturable adsorption process similar to Langmuir adsorption as the equilibrium which controls $[Cr^{VI}]$. One cannot rigorously exclude other mechanisms, but at least the results are consistent with Langmuir adsorption, and not with the solubility or depletion models. Based on the solution pH observed for Cr^{VI} release from a CCC or mixed oxide (4.6 ± 0.7), the fit shown in Fig. 9 corresponds to a β value of 10^7 - 10^{10} . Several observations about Eq. 3 and Fig. 9 deserve note. First, the agreement between the results from the CCC on different alloys and the synthetic mixed oxide implies that the same chemistry controls the release process. As stated previously,¹² we believe the CCC consists of a porous Cr^{III} - Cr^{VI} mixed oxide that can slowly release Cr^{VI} into solution. Second, there is a finite number of binding sites for Cr^{VI} on the insoluble Cr^{III} oxide matrix of a CCC, and the sites can be saturated. The high Cr^{VI} concentration and low pH present during CCC formation promotes Cr^{VI} adsorption and favors saturation of the matrix. Third, Cr^{VI} binding is strongly pH dependent, as is consistent with Fig. 6. The solid line in Fig. 6 was calculated from Eq. 3, and indicates reasonable agreement with experimental results. This dependence is a simple and predictable consequence of Reaction 1, in which high $[H^+]$ favors Cr^{VI} binding. Fourth, the equilibrium $[Cr^{VI}]$ has an unusual square-root dependence on N_{VI} (and therefore on the A/V ratio). Unlike a solubility mechanism, in which the solution reaches a saturation level, the $[Cr^{VI}]$ predicted from Eq. 3 increases with $(A/V)^{1/2}$ without bound. In reality, an upper limit of $[Cr^{VI}]$ will occur at saturation when a $Cr_2O_7^{2-}$ salt or CrO_3 precipitate, but this level is much higher (>0.1 M) than those observed during release experiments. In chemical terms, the square root dependence on A/V stems from the fact that the activity of adsorbed Cr^{VI} changes as release occurs, while the activity of a slightly soluble solid remains constant. Unlike the case for $SrCrO_4$ solubility, release of Cr^{VI} from the CCC affects both the Cr^{VI} activity in solution and adsorbed on the Cr^{III} matrix.

Solution of Eq. 2 for the case of an initial quantity of solid Cr^{III} hydroxide exposed to Cr^{VI} solution yields Eq. 4 (see Appendix for details)

$$[Cr^{VI}] = \frac{-z + \sqrt{z^2 + 4\beta[H^+][Cr^{VI}]_{t=0}}}{2\beta[H^+]} \quad [4]$$

$$z = 1 + \beta[H^+] \left(\frac{N_{VI}^{max}}{V} \right) - \beta[H^+][Cr^{VI}]_{t=0}$$

where N_{VI}^{max} is the moles of Cr^{VI} adsorbed to the Cr^{III} hydroxide at saturation, and $[Cr^{VI}]_{t=0}$ is the initial $[Cr^{VI}]$ in solution. The experimental results of Fig. 6 are consistent with Eq. 4 and Eq. 3, and a β value of 10^9 . For the results listed in Table II, there was significant variation in the equilibrium pH for different initial amounts of Cr^{III} hydroxide. The fairly wide spread of final pH values (about 3 pH units) prevented a reliable fit of the results to Eq. 4.

Implications to corrosion protection.—The current results provide additional support for previous conclusions about CCC chemistry, and add some new insights into chromate storage and release. The Langmuir adsorption model is completely consistent with Cr^{VI} storage in a CCC as a Cr^{III} - Cr^{VI} mixed oxide,¹² according to Reaction 1. The large binding constant of 10^7 - 10^{10} implies a strong bond between Cr^{III} and Cr^{VI} . For comparison, “chemisorption” is considered to have a ΔG° of adsorption more negative than -40 kJ/mol, corresponding to a binding constant of $>10^7$, while physisorption has a ΔG° above -25 kJ/mol ($\beta < 2 \times 10^4$).¹⁹ The β value estimated from Fig. 9 (10^7 - 10^{10}) corresponds to chemisorption, implying a relatively strong covalent bond. As noted earlier, the pH dependence of Cr^{VI} binding

apparent in Fig. 6 favors Cr^{VI} binding during CCC formation (low pH and high $[Cr^{VI}]$) and Cr^{VI} release in a defect in the field (low $[Cr^{VI}]$, neutral pH). The storage and release of Cr^{VI} is likely to be critical to the ability of chromate coatings to passivate defects, scratches, etc. While self-healing may also result from Cr^{VI} released by the $SrCrO_4$ containing primer, the two processes are controlled by different equilibria. The finite solubility of $SrCrO_4$ (~ 5 mM) implies that $SrCrO_4$ will dissolve until this limit is reached, perhaps leading to complete dissolution and depletion of the $SrCrO_4$ exposed to the environment. The Langmuir adsorption operative in the CCC does not result in a constant $[Cr^{VI}]$, but rather one that decreases as the CCC film is depleted. Although the released $[Cr^{VI}]$ decreases as the CCC is depleted, an equilibrium can be maintained at very low levels of both adsorbed and solution Cr^{VI} . Depending upon the $[Cr^{VI}]$ level required for self-healing, and the relative amounts of Cr^{VI} in CCC and primer, the CCC may outlast a $SrCrO_4$ primer, since the CCC will release less Cr^{VI} as it becomes depleted.

The effect of ionic strength on Cr^{VI} release is attributable to an activity effect. The activity coefficient calculated for $HCrO_4^-$ in 0.1 M NaCl quantitatively accounts for the higher equilibrium $[Cr^{VI}]$ in NaCl, at least to the accuracy expected from the extended Debye-Huckel equation.¹³ The current results do not take Cr^{VI} speciation into account, except for the spectrophotometric analysis described in Fig. 1 and 2. The distribution of solution Cr^{VI} between $HCrO_4^-$, CrO_7^{2-} , CrO_4^{2-} , and even H_2CrO_4 may affect the binding constant β . The dominant Cr^{VI} species in the conditions used here is $HCrO_4^-$, but the adsorption equilibria may vary above pH 6.5 or below pH 2. The value of β and the nature of the adsorbed Cr^{VI} may vary under these conditions, but Langmuir adsorption is still expected to prevail.

An additional issue of importance to the applications of CCCs involves aging after CCC formation. Aging of both the CCC on AA 2024-T3 and the Cr^{III} - Cr^{VI} mixed oxide for periods from 0.25 to 210 h at room temperature decreased the equilibrium $[Cr^{VI}]$ released into water (Table I). However, the decrease in Cr^{VI} release was not large; about 25% for the CCC and 40% for Cr^{III}/Cr^{VI} mixed oxide. A much greater decrease in Cr^{VI} release occurred after the CCC was heated at 50°C in air for 1 h. These decreases could be due to a reduction in CCC hydration or to a structural rearrangement that tightly binds Cr^{VI} .

In conclusion, the adsorption and release of Cr^{VI} from a CCC is consistent with adsorption of CrO_4^{2-} , $HCrO_4^-$ or $Cr_2O_7^{2-}$ to a porous, insoluble Cr^{III} hydroxide matrix. Adsorption is saturable, reversible, and pH dependent, with higher pH favoring desorption of Cr^{VI} . The low pH and relatively high $[Cr^{VI}]$ in a CCC formation path favor adsorption of Cr^{VI} to the Cr^{III} matrix formed by reduction of Cr^{VI} to the Cr^{III} by the alloy. The observations are quantitatively similar to a Langmuir adsorption-desorption equilibrium with a binding constant of 10^7 - 10^{10} for the Cr^{VI} interaction with Cr^{III} hydroxide. This high binding constant supports an adsorption mechanism based on formation of a covalent Cr^{III} -O- Cr^{VI} bond. Unlike traditional Langmuir adsorption to a surface, however, Cr^{VI} binding to Cr^{III} oxide occurs throughout the entire porous Cr^{III} film.

Acknowledgments

This work was supported by the Air Force Office of Scientific Research, contract F49620-96-1-0479. The authors wish to thank Martin Kendig for useful suggestions during the research.

The Ohio State University assisted in meeting the publication costs of this article.

Appendix

Release of Cr^{VI} from CCC.—Starting with Eq. 2 from the main text, we note that Γ_s is the initial coverage of Cr^{VI} in the CCC, (mol/cm²) and Γ_{VI} is the equilibrium coverage. Once equilibrium is reached

$$[Cr^{VI}] = \frac{(\Gamma_s - \Gamma_{VI})A}{V} \quad [A-1]$$

and

$$\Gamma_{VI} = \Gamma_s - [Cr^{VI}]V/A \quad [A-2]$$

since the released Cr^{VI} enters the solution as soluble Cr^{VI} . Substitution of Γ_{S} and Γ_{VI} from Eq. A-2 into Eq. 2 yields

$$[\text{Cr}^{\text{VI}}] + \frac{[\text{Cr}^{\text{VI}}]}{\beta[\text{H}^+]} - \frac{A\Gamma_{\text{S}}}{V\beta[\text{H}^+]} = 0 \quad [\text{A-3}]$$

Application of the quadratic formula and assignment of $\Gamma_{\text{S}}A$ as N_{VI} , the initial moles of Cr^{VI} in the CCC, yields Eq. 3 in the main text.

Release of Cr^{VI} from mixed oxide.—Solution of Eq. 2 for the $\text{Cr}^{\text{III}}/\text{Cr}^{\text{VI}}$ mixed oxide also yields Eq. 3, except the surface area of Cr^{III} in the solid is unknown. However, N_{VI} has the same meaning and can be calculated as the weight of oxide times the initial Cr^{VI} concentration in the oxide in terms of moles/gram.

Adsorption of Cr^{VI} to synthetic Cr^{III} hydroxide.—The area available for adsorption on the Cr^{III} hydroxide matrix is unknown, but is assumed to be proportional to the mass of Cr^{III} hydroxide, m , by some constant k , so that $A = km$. Starting with an initial Cr^{VI} in solution of $[\text{Cr}^{\text{VI}}]_{t=0}$, the equilibrium coverage of Cr^{VI} is

$$\Gamma_{\text{VI}} = \frac{([\text{Cr}^{\text{VI}}]_{t=0} - [\text{Cr}^{\text{VI}}])V}{mk} \quad [\text{A-4}]$$

Substitution of Γ_{VI} from Eq. A-4 into Eq. 2 yields

$$[\text{Cr}^{\text{VI}}]_{t=0} - [\text{Cr}^{\text{VI}}] = \frac{\beta[\text{Cr}^{\text{VI}}][\text{H}^+](\Gamma_{\text{max}}mk)}{(1 + \beta[\text{Cr}^{\text{VI}}][\text{H}^+])V} = 0 \quad [\text{A-5}]$$

Γ_{max} is the maximum loading of the Cr^{III} hydroxide, and differs from Γ_{S} for the CCC only in its relationship to microscopic rather than geometric area. The total moles of adsorbed Cr^{VI} , $N_{\text{VI}}^{\text{max}}$, is

$$N_{\text{VI}}^{\text{max}} = \Gamma_{\text{max}}mk \quad [\text{A-6}]$$

Substitution of Eq. A-6 into A-5 and solving for $[\text{Cr}^{\text{VI}}]$ yields Eq. 4 in the main text.

References

1. M. W. Kendig, A. J. Davenport, and H. S. Isaacs, *Corros. Sci.*, **34**, 41 (1993).
2. F. W. Lytle, R. B. Gregor, G. L. Bibbins, K. Y. Blohowiak, R. E. Smith, and G. D. Tuss, *Corros. Sci.*, **37**, 349 (1995).
3. H. Bohni and H. H. Uhlig, *J. Electrochem. Soc.*, **116**, 906 (1969).
4. S. T. Pride, J. R. Scully, and J. L. Hudson, *J. Electrochem. Soc.*, **141**, 3028 (1994).
5. F. Hunkeler and H. Bohni, *Corrosion*, **37**, 645 (1981).
6. H. A. Katzman, G. M. Malouf, R. Bauer, and G. W. Stupian, *Appl. Surf. Sci.*, **2**, 416 (1979).
7. J. Zhao, G. Frankel, and R. L. McCreery, *J. Electrochem. Soc.*, **145**, 2258, (1998).
8. A. L. Glass, *Mater. Prot.*, **7** (7) 27 (1968).
9. J. K. Hawkins, H. S. Isaacs, S. M. Heald, J. Tanquada, G. E. Thompson, and G. C. Wood, *Corros. Sci.*, **27**, 391(1987).
10. S. W. M. Chung, J. Robinson, G. E. Thompson, G. C. Wood, and H. S. Isaacs, *Philos. Mag. B.*, **63**, 557 (1991).
11. J. S. Wainwright, O. J. Murphy, and M. R. Antonio, *Corros. Sci.*, **33**, 281 (1992).
12. L. Xia and R. L. McCreery, *J. Electrochem. Soc.*, **145**, 3083 (1998).
13. D.C. Harris, *Quantitative Chemical Analysis*, 4th ed, pp. 186-188, W. H. Freeman, and Co., New York (1995).
14. V. G. Pouloupoulou, E. Vrachnou, S. Koinis, and D. Katakis, *Polyhedron*, **16**, 521 (1997).
15. J. J. Cruywagen, J. B. B. Heyns, and E. A. Rohwer, *Polyhedron*, **17**, 1741 (1998).
16. R. K. Tandon, P. T. Crisp, and J. Ellis, *Talanta*, **31**, 227 (1984).
17. T. Shen-Yang and L. Ke-An, *Talanta*, **33**, 775 (1986).
18. A. J. Bard and L. R. Faulkner, *Electrochemical Methods*, p. 516ff, Wiley, New York (1980).
19. P. Atkins, *Physical Chemistry*, 5th ed., p. 986, W. H. Freeman and Co., New York (1993).